

**(#3s) Rydberg states of cyclohexane, bicyclo[2.2.2]octane, and adamantane**

Q. Y. Shang and E. R. Bernstein

Citation: [The Journal of Chemical Physics](#) **100**, 8625 (1994); doi: 10.1063/1.466716

View online: <http://dx.doi.org/10.1063/1.466716>

View Table of Contents: <http://aip.scitation.org/toc/jcp/100/12>

Published by the [American Institute of Physics](#)

---

---

**COMPLETELY  
REDESIGNED!**



**PHYSICS  
TODAY**

*Physics Today* Buyer's Guide  
Search with a purpose.

# ( $\sigma$ 3s) Rydberg states of cyclohexane, bicyclo[2.2.2]octane, and adamantane

Q. Y. Shang<sup>a)</sup> and E. R. Bernstein

Department of Chemistry, Colorado State University, Fort Collins, Colorado 80523

(Received 26 November 1993; accepted 7 March 1994)

In this effort the effect of Rydberg electronic excitation on the structure of cyclic and polycyclic alkanes is investigated. Two-photon resonant, one-photon ionization, mass-resolved excitation spectroscopy is employed to observe the ( $\sigma$ 3s) $\leftarrow$ ( $\sigma$ )<sup>2</sup> Rydberg transitions of cyclohexane, bicyclo[2.2.2]octane, and adamantane cooled in a supersonic jet expansion. Rydberg spectra of these three molecules display sharp, well-resolved vibronic structure. Analysis of the spectra is assisted by isotopic substitution, circular/linear polarization, vibronic feature widths (rotational selection rules), as well as comparison to the ground-state vibrational energies. A significant reduction of vibrational energies in the excited electronic state and a 381 cm<sup>-1</sup> blue shift of the transition origin upon deuterium isotope substitution for cyclohexane are interpreted as due to the promotion of an electron from a  $\sigma$ -bonding orbital to a nonbonding Rydberg orbital upon optical excitation. Extensive vibronic coupling is observed for both cyclohexane and adamantane in their excited ( $\sigma$ 3s) Rydberg electronic states. Jahn-Teller splitting is small for adamantane but quite substantial for cyclohexane. This difference is attributed to the basic stability difference for the two different ring systems (mono- and tri-cyclic). A progression in a nontotally symmetric mode is observed in the Rydberg spectrum of bicyclo[2.2.2]octane suggesting a change in the geometry of this molecule upon ( $\sigma$ 3s) $\leftarrow$ ( $\sigma$ )<sup>2</sup> excitation.

## I. INTRODUCTION

Despite the ubiquity and importance of alkanes, their electronic spectroscopy, and consequently their electronic structure, are far less well known and understood than their conjugated or aromatic counterparts. The one-photon allowed electronic spectra of alkanes are broad and devoid of molecular information.<sup>1</sup> In general, two types of electronic transitions are expected for an alkane molecule: electronic excitations from a bonding  $\sigma$  orbital to an antibonding  $\sigma^*$  orbital; and electronic excitations from a bonding  $\sigma$  orbital to a nonbonding Rydberg ( $n > 2$ ) orbital. Various suggestions have been advanced to account for the diffuseness of the ( $\sigma\sigma^*$ ) $\leftarrow$ ( $\sigma$ )<sup>2</sup> valence (bonding-antibonding) transitions.<sup>1</sup> The three most obvious ones are Franck-Condon displacements in the excited antibonding state, predissociation of the excited state due to C-C bond weakening, and multiple conformations for longer chain systems. Even small linear alkanes show little resolved structure.<sup>2</sup> Cyclic systems do, however, evidence well-resolved Rydberg spectra.<sup>2,3</sup> A series of Rydberg states ( $ns, np, nd$ ) has been identified for cyclohexane, bicyclo[2.2.2]octane, and adamantane.<sup>4</sup>

Vibronic structure is often observed in the Rydberg transition of cyclic and polycyclic alkanes.<sup>4</sup> These vibronic features are typically quite similar for different Rydberg states because the Rydberg electron is nonbonding and the remaining "core" electronic system is the same for the Rydberg states. These features have not been carefully or completely analyzed in the past due to the limited resolution of one-photon absorption spectroscopy above 50 000 cm<sup>-1</sup>, spectral congestion, and potential Jahn-Teller vibronic activity.

Robin and co-workers<sup>5</sup> have probed the lower-lying

Rydberg transitions of cyclic and polycyclic alkanes via two-photon resonant, multiphoton ionization spectroscopy (electron detection) in a static room temperature gas cell. Transitions observed are in the ultraviolet and are assigned as ( $\sigma$ 3s) $\leftarrow$ ( $\sigma$ )<sup>2</sup>. Vibronic structure is partially resolved on many of these transitions; however, a detailed vibronic interpretation of these spectra is complicated by the presence of hot bands and a limited range of available laser wavelengths.

A detailed vibronic analysis of ( $\sigma$ 3s) $\leftarrow$ ( $\sigma$ )<sup>2</sup> Rydberg spectra of cyclic and polycyclic alkanes would be of considerable interest and utility for a number of reasons: (1) vibronic structure of ( $\sigma$ 3s) $\leftarrow$ ( $\sigma$ )<sup>2</sup> transitions can be representative of that found for many different Rydberg transitions;<sup>4</sup> (2) these transitions can result in a significant change of bonding character for the molecule and thus may generate large changes in selected vibrational frequencies;<sup>1</sup> (3) many of these transitions are potentially Jahn-Teller active and are expected to show strong vibronic coupling effects; and (4) cyclic and polycyclic alkane structures have important applications for fundamental issues in synthetic and energetic materials chemistry.<sup>6</sup> Studies of these model systems (cyclohexane, bicyclo[2.2.2]octane, and adamantane) will help elucidate the stability and chemical reactivity of the Rydberg states of caged structures in general.

In this paper, the two-photon resonant, multiphoton ionization, mass-resolved excitation spectrum of cyclohexane (C<sub>6</sub>H<sub>12</sub>), bicyclo[2.2.2]octane (C<sub>8</sub>H<sub>14</sub>), and adamantane (C<sub>10</sub>H<sub>16</sub>) for the ( $\sigma$ 3s) $\leftarrow$ ( $\sigma$ )<sup>2</sup> Rydberg transition are reported. The molecules are cooled in a supersonic expansion to alleviate the problem of hot band interference in the data analysis. Vibronic features are partially assigned with the help of H/D isotopic substitution and laser polarization ratio studies, as feasible. The observed vibronic structures are interpreted based on selection rules, polarization effects, lin-

<sup>a)</sup>Current address: Applied Materials, Santa Clara, California.

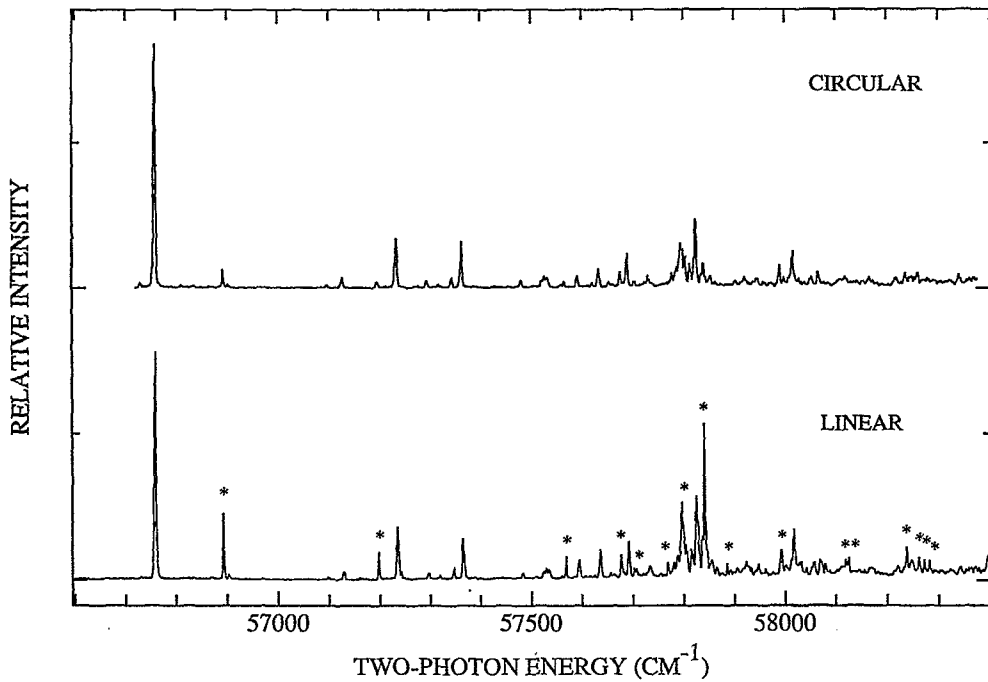


FIG. 1. Mass-resolved, two-photon resonance enhanced, multiphoton ionization spectrum of cyclohexane- $h_{12}$  [ $(\sigma 3s) \leftarrow (\sigma)^2$ ] in both linearly and circularly polarized light. The signal above  $58\ 400\text{ cm}^{-1}$  is very weak and devoid of any sharp structure. Features marked with \* have a very narrow linewidth ( $\sim 0.4\text{ cm}^{-1}$ ) and a circular to linear polarization intensity ratio  $W$  less than 1. The intensity of these two traces is adjusted so that the origin intensity is the same in both of them. Actually  $I_{\text{cir}}/I_{\text{lin}} \sim 3/2$  for the  $0_0^0$  transition. See Table I for a tabulation of transitions.

ewidths (rotational structure), isotope effects, Jahn-Teller activity, and of course, mass selection of the absorbing species.

## II. EXPERIMENTAL PROCEDURES

Mass-resolved two-photon excitation, one- or multiphoton ionization spectroscopy (MRES, in general) has been described in this context previously.<sup>7</sup> Mass detected spectroscopy is useful in this instance for two reasons: (1) emission from these samples would appear below  $2000\text{ \AA}$ —a difficult spectral region for photomultiplier tubes; and (2) mass-resolved spectra insure against misinterpretations due to impurity and cluster features. Samples are placed in a pulsed nozzle and pressurized with an expansion gas of 90% He and 10% CH<sub>4</sub>. This mixture is found to generate maximum cooling for the sample molecules without reducing the overall bare molecule signal. The nozzle is heated to 150 °C for adamantane, 120 °C for bicyclooctane, and 30 °C for cyclohexane. Cyclohexane- $h_{12}$  and adamantane are obtained from Aldrich Chemical Co., cyclohexane- $d_{12}$  from Cambridge Isotope Co., and bicyclooctane from Wiley Organics Co. Laser excitation is provided by a Nd/YAG pumped (10 Hz) dye laser whose output can be frequency doubled or mixed with the 1.064  $\mu\text{m}$  YAG fundamental to obtain the desired photon wavelength. A 30 cm lens is used to focus the laser beam onto the molecular beam. Spectra are typically collected at  $0.4\text{ cm}^{-1}$  resolution, but some spectra (as indicated) are obtained with a laser resolution of  $0.14\text{ cm}^{-1}$ .

Both linearly and circularly polarized light are employed to collect spectra in order to help identify the symmetry of

the observed transitions for cyclohexane and adamantane. The output of the laser is employed with a linear polarizer to generate the linearly polarized spectral data. Circular polarization is achieved by further passing this light through a Fresnel rhomb (CVI Laser Co.). At this time, the features of the spectrum of bicyclooctane are too weak to derive accurate polarization ratios.

## III. RESULTS AND DISCUSSION

### A. General considerations

The point groups that are important for analysis of the presented data are  $D_{3d}$  (cyclohexane),  $D_{3h}$  (bicyclooctane), and  $T_d$  (adamantane). The one-photon selection rules for these point groups can be found in Refs. 7(a), 8, and 9 and the two-photon selection rules and tensor elements can be found in Refs. 7(a) and 10. The original references to the development of two-photon spectroscopy are presented in Ref. 10.

In discussing the spectroscopic results presented in this report, we treat the three-photon ionization spectroscopic transitions by two-photon selection rules. The resonant two-photon step controls the symmetry behavior of the transitions because the  $I \leftarrow A$  transition is between different species and of a nonresonant nature.<sup>7(a)</sup>

### B. $(\sigma 3s) \leftarrow (\sigma)^2$ Rydberg transition of cyclohexane

#### 1. Two-photon excitation of C<sub>6</sub>H<sub>12</sub>

Figure 1 displays the mass-resolved excitation spectrum of C<sub>6</sub>H<sub>12</sub> taken with both linearly and circularly polarized

laser light. Relative peak intensity has been adjusted to give the  $I_{\text{cir}}/I_{\text{lin}}=1$  for the  $0_0^0$  transition. The scanning (one-photon) resolution of the laser is roughly  $0.2 \text{ cm}^{-1}$ . The laser is tuned from 27 300 to 29 630  $\text{cm}^{-1}$ . The first observed feature appears at  $28\ 379 \text{ cm}^{-1}$  and is assigned as the  $0_0^0$  transition ( $56\ 758 \text{ cm}^{-1}$ ) of cyclohexane- $h_{12}$ . The ionization threshold for this molecule lies at  $78\ 682 \text{ cm}^{-1}$ <sup>11</sup> and thus the overall spectroscopic plus detection process requires three photons [(2+1) resonance enhanced ionization]. So many features are observed in this spectrum that a complete assignment is not presently possible. Table I lists the major observed peaks in this spectrum at their two-photon energy.

From Fig. 1 we note that two different types of features are observed in the spectrum: features not marked with \* in this figure (e.g.,  $0_0^0$ ) have a  $\sim 2 \text{ cm}^{-1}$  width and a circular to linear polarization intensity ratio greater than 1; and features marked with an \* (e.g.,  $56\ 894 \text{ cm}^{-1}$ ) which have a  $0.4 \text{ cm}^{-1}$  width and a polarization intensity ratio (circular/linear) less than 1. Figure 2 demonstrates this linewidth (which consists of unresolved rotational structure) difference quite clearly for a laser linewidth of  $0.07 \text{ cm}^{-1}$ .

## 2. Two-photon excitation of $C_6D_{12}$

The two-photon mass-resolved excitation of  $C_6D_{12}$  is presented in Fig. 3. This sample is investigated as an aid to making vibrational assignments in the cyclohexane- $h_{12}$  spectrum. The observed features are tabulated and presented in Table II which is arranged in the same fashion as Table I. The  $0_0^0$  transition for  $C_6D_{12}$  is  $+381 \text{ cm}^{-1}$  higher in energy than that for  $C_6H_{12}$ : the vibrational frequencies have thus decreased significantly in the excited state with respect to those of the ground state. This result is consistent with the expectation that the promotion of an electron from a  $\sigma$  bonding orbital to a nonbonding Rydberg orbital occurs upon optical electronic excitation. In all other respects (e.g., linewidths, polarization ratios, number of features observed, etc.) the two spectra ( $C_6D_{12}$ ,  $C_6H_{12}$ ) are very similar.

## 3. Vibronic analysis

Since the chair conformation of cyclohexane is 7.8 kcal/mol more stable than the boat conformation<sup>12</sup> and the nozzle is below  $30^\circ\text{C}$  for the cyclohexane expansion, we assume in the ensuing discussion that only the chair conformation is present in the beam.

Electronic state symmetry—Chair cyclohexane has  $D_{3d}$  symmetry in its ground state. Our *ab initio* calculation (RHF with a DZV basis set augmented with two  $3s$  functions for each carbon atom) gives the HOMO as  $e_g$  and the LUMO as  $a_{1g}$  (predominantly  $3s$  in character). Thus the transition  $3s(a_{1g}) \leftarrow e_g$  has an overall electronic symmetry of  $E_g \leftarrow A_{1g}$ . The observed two-photon excitation can be assigned to this symmetry based on the following reasoning: (1) it is the lowest observed sharp transition;<sup>4</sup> (2) its term value,  $22\ 924 \text{ cm}^{-1}$  [calculated as  $E(\text{ionization}) - E(\text{excitation})$ ], is consistent with the  $3s$  orbital;<sup>1</sup> (3) *ab initio* calculation suggests the unoccupied  $\sigma^*$  orbital is much higher in energy than the LUMO  $3s$  orbital; and (4) the transition is one-photon forbidden and two-photon

TABLE I. List of major peaks observed in two-photon MRES of cyclohexane- $h_{12}$  given in  $\text{cm}^{-1}$ .

Vibronic features <sup>a</sup>		Assignments, isotope ratio <sup>b</sup>
Energy	Intensity	
0	s	$0_0^0, 56\ 758$
136*	s	
372	w	$\nu_6(384), 1.35(1.28)$
440*	m	
478	m	
540	vw	
564	vw	
590	w	
608	m	$\nu_5(802), 1.14(1.10)$
726	vw	
768	vw	
772	w	
778	vw	
812*	m	$440 + \nu_6$
838	m	
880	m	
920*	m	
934	m	
948*	w	
976	m	
1012*	w	
1024	vw	
1030	vw	
1040*	s	$440 + \nu_5$
1048	w	
1058	w	
1068	s	$\nu_4(1158), 1.17(1.14)$
1084*	s	
1098	vw	
1128*	vw	
1168	w	
1190	vw	
1236*	m	
1262	m	$\nu_3(1465), 1.21(1.3)$
1272	w	
1300	w	
1314	w	
1324	w	
1362*	vw	
1368*	vw	
1480*	m	$440 + \nu_4$
1496	w	
1504*	w	
1514*	w	
1524*	w	
1638	w	

<sup>a</sup>Features marked with \* have a  $0.4 \text{ cm}^{-1}$  linewidth and a circular to linear polarization intensity ratio less than 1. See Figs. 1 and 2.

<sup>b</sup>Values in parentheses are ground-state numbers for vibrational energies and isotopic ratios  $\nu(\text{H}_{12})/\nu(\text{D}_{12})$ .

allowed.<sup>8,9</sup> Comparison of the one-photon<sup>4</sup> and two-photon spectra shows that the first one-photon feature is  $372 \text{ cm}^{-1}$  higher in energy than the two-photon origin characterized in this study. This one-photon feature is probably a vibronic origin associated with an  $a_{2u}$  mode (ground state  $522 \text{ cm}^{-1}$ ),<sup>8,9</sup> although an  $e_u$  mode would also generate one-photon intensity ( $e_u \times E_g = A_{1u} + A_{2u} + E_u$ ). Previously reported features at lower energies must be associated with hot band structure as they are not observed under cold conditions.<sup>5</sup>

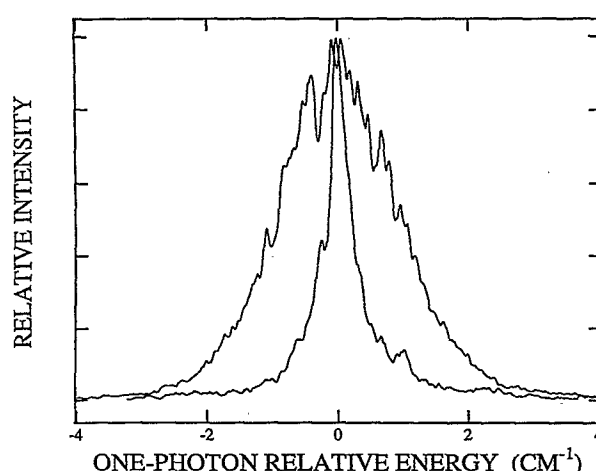


FIG. 2. Expanded view of mass-resolved, two-photon resonance enhanced, multiphoton ionization spectrum of cyclohexane- $h_{12}$  for peaks at 56 758 (0<sub>0</sub><sup>g</sup> transition—broad) and 56 894 (vibronic transition—narrow)  $\text{cm}^{-1}$  obtained with linearly polarized light. Laser resolution is 0.07  $\text{cm}^{-1}$ . These features also have different polarization ratios as can be seen in Fig. 1.

Vibronic symmetry—The  $D_{3d}$  cyclohexane molecule has six totally symmetric modes. Since many more peaks are observed in the spectra of this molecule, and combination and overtone intensity does not appear to be a reasonable assignment for most of the features, other modes must be present in the spectra.

In addition to  $A_{1g}$  modes,  $e_g$  modes can be vibronically active in an  $E_g$  electronic transition:

$$e_g \times E_g = A_{1g} + A_{2g} + E_g.$$

Vibronic transitions to both  $A_{1g}$  and  $E_g$  symmetry states are allowed in this experiment. Transitions to the  $A_{2g}$  vibronic state would be allowed if the two-photon transition were induced by photons of different energy.<sup>10</sup> Additionally, the three vibronic states generated by the  $e_g \times E_g$  vibronic coupling could have different energies if the coupling terms are large (Jahn-Teller effect).<sup>9</sup> The  $A_{1g}$  component is expected at lower energy than the  $E_g$  component.<sup>9</sup>

The two two-photon allowed components of the ( $E_g \times e_g$ ) vibronic couple  $A_{1g}$  and  $E_g$  can be distinguished through their polarization behavior,<sup>10</sup>

$$W = I_{\text{cir}} / I_{\text{lin}}.$$

$I_{\text{cir}}$  and  $I_{\text{lin}}$  are the peak intensities in the spectrum obtained with circularly and linearly polarized light, respectively:  $W$  is less than 1 for the transition to an  $A_{1g}$  vibronic component; and  $W$  equals 3/2 for the transition to an  $E_g$  vibronic component.<sup>10</sup>

In addition, the linewidth and/or shape of the observed spectral features (which are governed by unresolved rotational structure) may be different for the two types of vibronic transitions because the rotational selection rules are different for them. Rotational selection rules for two-photon transitions are discussed in Ref. 10. For a molecule with  $D_{3d}$  symmetry,  $\Delta K=0$ ,  $\Delta J=0, \pm 1, \pm 2$  for  $A_{1g} \leftarrow A_{1g}$  vibronic

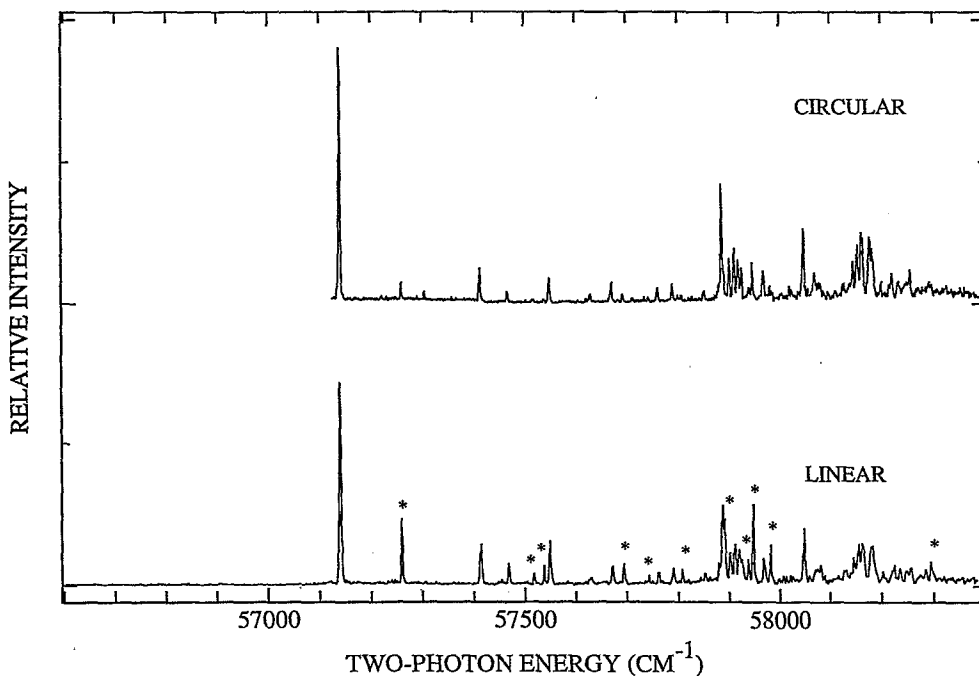


FIG. 3. Mass-resolved, two-photon resonance enhanced, multiphoton ionization spectrum of cyclohexane- $d_{12}$  [ $(\sigma_{3s}) \leftarrow (\sigma)^2$ ] obtained with both linearly and circularly polarized light. See Table II for peak positions and assignments. See caption for Fig. 1 for further information.

TABLE II. The observed major vibronic peaks in two-photon MRES of cyclohexane-*d*<sub>12</sub> given in cm<sup>-1</sup>.

Vibronic features <sup>a</sup>		Assignments, isotope ratio <sup>b</sup>
Energy	Intensity	
0	s	0 <sub>0</sub> <sup>0</sup> , 57 137
120*	s	
274	m	$\nu_6(298)$
328	w	
378*	w	
398*	w	
410	m	
490	vw	
532	w	$\nu_5(727)$
554*	w	
602*	w	
622	w	
652	w	
668*	w	$398 + \nu_6$
746	w	
752*	s	
762	m	
770	m	
780	m	
786	w	
798*	w	
808*	s	
828	w	
842*	s	
910	s	$\nu_4(1013)$
930	w	
942	vw	
988	vw	
1006	m	
1014	m	
1022	m	
1027	m	
1040	m	
1044	m	
1086	w	
1098	w	
1116	w	
1154*	w	

<sup>a</sup>Features marked with \* have a 0.4 cm<sup>-1</sup> linewidth and a circular to linear polarization intensity ratio less than 1. See Figs. 1 and 2.

<sup>b</sup>Values in parentheses are ground-state numbers for vibrational energies.

transitions, and  $\Delta K = \pm 1, \pm 2$ ,  $\Delta J = 0, \pm 1, \pm 2$  for  $E_g \leftarrow A_{1g}$  vibronic transitions. MOPAC semiempirical calculations<sup>15</sup> for the ground state find C<sub>6</sub>H<sub>12</sub> rotational constants are  $A = B = 0.14$  cm<sup>-1</sup> and  $C = 0.08$  cm<sup>-1</sup>. Based on these selection rules and rotational constants, one predicts that the rotational structure on these vibronic transitions will not be resolved at 0.07 cm<sup>-1</sup> one-photon resolution; however, the  $A_{1g} \leftarrow A_{1g}$  transition linewidths (rotational contours) should be narrower than those for the  $E_g \leftarrow A_{1g}$  transitions due to more stringent and restrictive selections. Contour calculations confirm this assertion for a laser resolution  $\sim 0.1$  cm<sup>-1</sup>. Specifically, the  $\Delta J = 0$   $\Delta K = 0$  transitions for  $A_{1g} \leftarrow A_{1g}$  vibronic transitions have an intense, sharp unresolved *Q* branch if one assumes that  $A', B', C'$  are roughly equal to  $A'', B'', C''$ , that the centrifuged distortion constant  $\zeta$  is small in both states, and that the rotational temperature is  $\sim 5$  K.  $\Delta K = 0$   $\Delta J = \pm 1, \pm 2$  transitions add a weak and broad structure approxi-

mately symmetrically about this sharp feature, as is observed. The  $E_g \leftarrow A_{1g}$  vibronic transitions display no intense central feature, just a dense set of transitions about the vibronic origin where intensity is governed by the  $\sim 5$  K Boltzmann population of the ground state. The  $E_g \leftarrow A_{1g}$  band shapes are also expected to be roughly symmetrical for the observed transitions. Both features are about a factor of 2 sharper than would be expected based on the above assumptions concerning  $A$ ,  $B$ ,  $C$ ,  $\zeta$ , and  $T_{\text{rot}}$ . This suggests that  $A', B', C', \zeta \neq A'', B'', C'' \zeta''$  and/or that  $T_{\text{rot}} < 5$  K, and that dynamical effects do not govern the observed transition widths.

To summarize this discussion,  $e_g$  vibrational modes can be vibronically active in an  $E_{1g} \leftarrow A_{1g}$  transition. Two vibronic components of an  $e_g \times E_g$  couple can be observed by two-photon (same energy) spectroscopy. The three components of  $e_g \times E_g$  ( $A_{1g}, A_{2g}, E_g$ ) can additionally be removed in energy from one another if Jahn-Teller vibronic matrix elements are nonzero. The  $A_{1g}$  and  $E_g$  vibronic components of this coupling can be differentiated and assigned through linear and circular polarization excitation studies [ $I_{\text{cir}}/I_{\text{lin}}(A_{1g}) < 1$  and  $I_{\text{cir}}/I_{\text{lin}}(E_g) = 3/2$ ] and through linewidth ( $\Delta\nu$ ) studies [ $\Delta\nu(A_{1g}) < \Delta\nu(E_g)$ ].

Thereby, based on the above reasoning, the peaks in the C<sub>6</sub>H<sub>12</sub>/C<sub>6</sub>D<sub>12</sub> spectra with both narrow widths ( $\Delta\nu < 1$  cm<sup>-1</sup>, Fig. 2) and a significant relative intensity decrease in circularly polarized laser radiation (Figs. 1 and 3) can be identified as  $A_{1g}$  vibronic states in the  $E_g$  excited Rydberg state arising from  $e_g \times E_g$  vibronic coupling. Moreover, because of peakwidth and intensity one knows that the Jahn-Teller activity within these  $e_g \times E_g$  couples is significant because such unique behavior is indeed observed. A total of 16 such peaks can be identified in the C<sub>6</sub>H<sub>12</sub> spectrum: 136, 440, 812, 920, 948, 1012, 1040, 1084, 1128, 1236, 1362, 1368, 1480, 1504, 1514, 1524 cm<sup>-1</sup> (see Table I). These features are in general quite intense. Eleven such modes can be identified in the C<sub>6</sub>D<sub>12</sub> spectrum: 120, 378, 398, 554, 602, 668, 752, 798, 808, 842, 1154 cm<sup>-1</sup> (Table II). Again a significant Jahn-Teller activity is consequently indicated for C<sub>6</sub>D<sub>12</sub>.

The totally symmetric  $a_{1g}$  vibrational modes should have  $E_g$  overall vibronic symmetry in an  $E_g$  electronic state. Thus the  $E_g$  two-photon allowed features in this spectrum should have two sources:  $e_g \times E_g$  Jahn-Teller derived vibronic features and  $a_{1g} \times E_g$  vibronic features. All features in the spectrum not marked with \* have a large linewidth ( $\Delta\nu \sim 4$  cm<sup>-1</sup>) and  $I_{\text{cir}}/I_{\text{lin}} > 1$  (see Figs. 1 and 3). As can be seen from the figures, many more than the six  $a_{1g}$  fundamental modes ( $E_g$  vibronic states) are present in the C<sub>6</sub>H<sub>12</sub> and C<sub>6</sub>D<sub>12</sub> spectra.

**Totally symmetric modes**—As pointed out above, cyclohexane has only six totally symmetric ground-state vibrations. The modes of  $a_{1g}$  symmetry and their ground-state energies (H<sub>12</sub>/D<sub>12</sub>) are 2936/2150 ( $\nu_1$ ), 2853/2081 ( $\nu_2$ ), 1465/1119 ( $\nu_3$ ), 1158/1013 ( $\nu_4$ ), 802/723 ( $\nu_5$ ), and 384/298 ( $\nu_6$ ).<sup>14</sup> The  $\nu_1$  and  $\nu_2$  C-H stretching modes will probably not be seen in the reported spectra because of the energy accessed. Thus only four  $a_{1g}$  fundamental modes plus their overtones and combinations should appear in these spectra. If we assume that the isotope ratio for these modes is similar in both the ground and excited electronic states and that these modes

should be reduced in energy in the excited state, a reasonable assignment for the remaining four totally symmetric modes can be suggested. We assign features at 372/274, 608/532, and 1069/910  $\text{cm}^{-1}$  to  $\nu_6, \nu_5, \nu_4$  ( $\text{H}_{12}/\text{D}_{12}$ ), respectively. Their isotopic ratios are 1.35, 1.14, and 1.17 in the excited  $E_g$  Rydberg state compared to 1.28, 1.10, and 1.14, respectively, in the  $A_{1g}$  ground state. Based on these fundamentals,  $2\nu_6$ ,  $\nu_6 + \nu_5$ , and  $2\nu_5$  can be identified in the spectrum of  $\text{C}_6\text{H}_{12}$ .

Vibronically active  $e_g$  modes—One knows from the large number of  $E_g$  vibronic features (broad lines and polarization behavior) in the spectrum of cyclohexane that the  $e_g \times E_g$  Jahn-Teller coupling is substantial and the  $E_g$  vibronic states thus derived are different in energy from the  $A_{1g}$  and  $A_{2g}$  components. The  $A_{1g}$  vibronic components are marked in the tables and figures with an asterisk. In the ground state the  $e_g$  fundamental modes are found at 2924, 2895, 1445, 1347, 1268, 1029, 758, 427  $\text{cm}^{-1}$ . These modes do not readily correlate with any of the \* marked modes; therefore, the Jahn-Teller coupling and splitting of the  $e_g \times E_g$  vibronic couple is substantial. Moreover, many more  $E_g$  features are identified than are possible from  $e_g$  fundamental modes. This suggests that overtones and combinations of  $e_g$  modes also play a role in the vibronic coupling in this excited  $E_g$  electronic state. The vibronic coupling problem for this system is thus quite complicated. We have made some assignments in Tables I and II that arise from an  $A_{1g}$  vibronic mode in combination with an  $a_{1g}$  fundamental vibrational mode. Additional complications can arise from overtone/combination splitting of  $e_g$  modes due to anharmonicities not directly related to the Jahn-Teller coupling in this state.

We can summarize the situation depicted for the cyclohexane Rydberg transition as follows: (1) the transition is  $E_g \leftarrow A_{1g}[(\sigma 3s) \leftarrow (\sigma)^2]$ ; (2) four totally symmetric modes are assigned in the excited state; (3) 16 peaks in the spectrum have  $I_{\text{cir}}/I_{\text{lin}}$  and linewidths that are different from the  $0_0^0$  transition and these are assigned as the  $A_{1g}$  Jahn-Teller vibronic components of  $e_g \times E_g$  vibronic coupling within the excited electronic state; and (4) extensive Jahn-Teller and other vibronic coupling interactions are present in the  $E_g$  Rydberg state. Two reasons can be cited for the extensive and large Jahn-Teller coupling observed: (1) the degeneracy occurs for the HOMO  $\sigma$  bonding orbital; and (2) the cyclohexane ring is not very rigid.

### C. $(\sigma 3s) \leftarrow (\sigma)^2$ Rydberg transition of bicyclo[2.2.2]octane(BCO)

Figure 4 displays the (2+1) mass-resolved excitation spectrum of BCO monitored in the BCO mass channel. The signal is quite weak, at least ten times weaker than that measured for cyclohexane, under similar circumstances. No other signals are found for this molecule in the range 26 065 to 27 255  $\text{cm}^{-1}$  (one-photon energy). The ionization energy for BCO is 76 052  $\text{cm}^{-1}$ ; one derives from the spectrum that the process is indeed a (2+1) ionization as the laser fundamental is scanned. Only five peaks are observed as a progression in roughly 60  $\text{cm}^{-1}$ . These features are tabulated in Table III. The observed features are not hot bands and the spectrum of

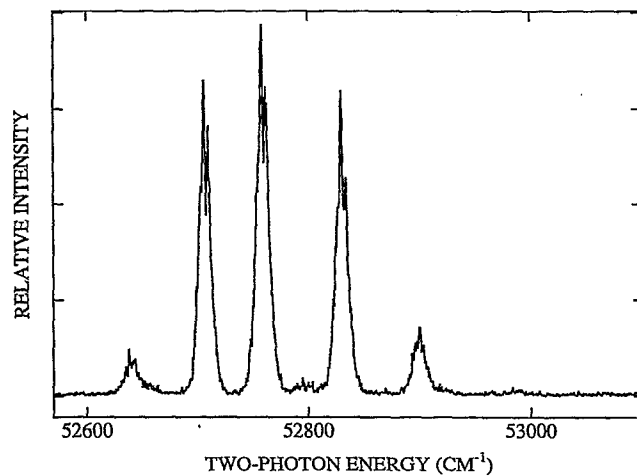


FIG. 4. Mass-resolved, two-photon resonance enhanced, multiphoton ionization spectrum of bicyclo[2.2.2]octane  $[(\sigma 3s) \leftarrow (\sigma)^2]$ . The origin is at 52 707  $\text{cm}^{-1}$ . The signal above 53 200  $\text{cm}^{-1}$  is weak and no sharp structure is found. See Table III for peak positions. Spectrum taken with linearly polarized laser light.

BCO is uncongested and comparatively well-resolved. Potential assignments for these features are presented below.

BCO has  $D_{3h}$  ground-state symmetry. Based on a previously reported calculation,<sup>16</sup> two occupied orbitals (HOMO,  $\sigma$ ),  $4e''$  and  $6a'_1$ , are accidentally degenerate; the LUMO orbital is of  $a'_1$  symmetry and largely composed of  $3s$  atomic carbon orbitals. Since the transition energy is similar to that for cyclohexane we assume the transition is  $(\sigma 3s) \leftarrow (\sigma)^2$ . The transition can be either  $E'' \leftarrow A'_1$  or  $A'_1 \leftarrow A'_1$  in nature. Both possibilities are one-photon forbidden and two-photon allowed. The reported one-photon spectrum begins near 58 100  $\text{cm}^{-1}$ .<sup>4</sup>

One could distinguish between these two possible excited-state symmetries by polarization studies:  $W=3/2$  for the  $E'' \leftarrow A'_1 0_0^0$  transition and  $W<1$  for the  $A'_1 \leftarrow A'_1 0_0^0$  transition.<sup>10</sup> Unfortunately, these features (and indeed the entire spectrum) are quite weak and good polarization intensity ratio studies are difficult to generate. We are thus not able to decide this assignment based on  $W$  at this time.

Nonetheless, one can still discuss the nature of the observed progression in a low-frequency mode. The molecule is certainly displaced in the  $(\sigma 3s)$  Rydberg state along a particular molecular coordinate. A ground-state skeletal

TABLE III. List of major peaks in two-photon MRES of bicyclo[2.2.2]octane in  $\text{cm}^{-1}$ .

Vibronic features <sup>a</sup>
0 (52 638, 0 <sup>b</sup> )
60
121
193
263
350

<sup>a</sup>See the text for vibronic assignment possibilities—progression in  $a''_1$  mode (65  $\text{cm}^{-1}$  in ground state).

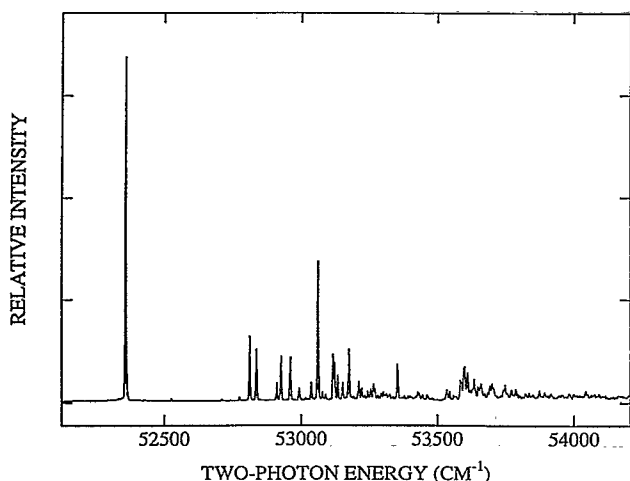


FIG. 5. Mass-resolved, two-photon resonance enhanced, multiphoton ionization spectrum of adamandane [ $(\sigma 3s) \leftarrow (\sigma)^2$ ] obtained with linearly polarized light. The origin is at  $52\ 358\ \text{cm}^{-1}$ . The signal above  $54\ 000\ \text{cm}^{-1}$  is broad and weak. See Table IV for peak positions.

mode for  $a''_1$  symmetry is calculated at  $65\ \text{cm}^{-1}$ .<sup>17</sup> If the excited electronic state is of  $E''$  symmetry this mode could be the progression forming ( $n=0, 1, 2, 3, 4$ ) one at  $\sim 60\ \text{cm}^{-1}$  in the excited electronic state. If the excited electronic state is of  $A'_1$  symmetry, this mode could be the progression forming one ( $n=0, 2, 4, 6, 8$ ) at  $\sim 30\ \text{cm}^{-1}$  in the excited electronic. A more detailed analysis must await better *ab initio* calculations.

#### D. $(\sigma 3s) \leftarrow (\sigma)^2$ Rydberg transition of adamantane

Figure 5 presents the (2+1) mass-resolved excitation spectrum of adamantane for the  $(\sigma 3s) \leftarrow (\sigma)^2$  Rydberg transition near  $52\ 500\ \text{cm}^{-1}$ . The spectrum is scanned from  $25\ 725$  to  $27\ 255\ \text{cm}^{-1}$ . The spectrum to higher energy than this is both broad and weak. The  $0^0_0$  transition for this region lies at  $26\ 179\ \text{cm}^{-1}$  (one-photon energy). The ionization energy for adamantane lies at  $74\ 600\ \text{cm}^{-1}$ .<sup>11</sup> The features in the spectrum are tabulated in Table IV. The vibronic features are well-resolved and no hot band features are observed in this spectrum.<sup>5</sup>

The point group of ground-state adamantane is  $T_d$ . According to Robin *et al.*<sup>5</sup> the transition must be assigned as  $T_2 \leftarrow A_1$  since this excited-state symmetry is the only one possible for both one- and two-photon allowed transitions in  $T_d$  symmetry. The transition energy and term value are as expected for a  $(\sigma 3s) \leftarrow (\sigma)^2$  Rydberg transition. The experimental assignment for the transition is consistent with the calculated HOMO and LUMO estimates.<sup>18</sup>

Totally symmetric vibrations can be expected to accompany the origin transition; according to the results of ground-state vibrational analysis, five totally symmetric vibrations ( $a_1$ ) are expected for adamantane and they are assigned at 746, 969, 1453, 2856, and  $2909\ \text{cm}^{-1}$ .<sup>19</sup> The last two of these are C-H stretching modes and are probably not observed within the presented energy range in Fig. 5 and Table

TABLE IV. List of major peaks observed in two-photon MRES of adamantane in  $\text{cm}^{-1}$ .

Vibronic features		
Energy	Intensity	Assignments
0	s	$0^0_0, 52\ 359$
412	w	
450	m	
476	m	
554	w	
568	m	
600	m	
634	w	
679	w	
702	s	
720	vw	$\nu_5(756)$
730	vw	
760	m	
764	m	
776	w	
794	w	
817	m	$\nu_4(969)$
853	w	
863	w	
885	vw	
897	w	
907	w	
912	w	
923	vw	
934	vw	
943	vw	
994	m	
1071	vw	
1087	vw	
1103	vw	
1176	w	
1187	w	
1227	w	
1241	m	
1256	m	
1277	w	$\nu_3(1453)$

IV. We assign the excited-state modes  $702(\nu_5)$ ,  $817(\nu_4)$ , and  $1256(\nu_3)$   $\text{cm}^{-1}$  based entirely on the frequency match to the ground-state modes.

Additionally,  $e$ ,  $t_1$ , and  $t_2$  modes can also be active for two-photon (and one-photon) spectroscopy in the  $T_2$  electronic state:

$$e \times T_2 = T_1 + T_2,$$

$$t_1 \times T_2 = A_2 + E + T_1 + T_2,$$

$$t_2 \times T_2 = A_1 + E + T_1 + T_2.$$

$A_1$ ,  $E$ , and  $T_2$  vibronic states are all two-photon allowed from the  $A_1$  ground state,  $e$  and  $t_2$  modes are Jahn-Teller active<sup>9</sup> ( $[T_2 \times T_2 \times t_1]$  does not contain  $A_1$ ), and  $A_2$  states are not observed in either one- or two-photon transitions. Additionally,  $t_1$  modes can cause splittings of the  $(t_1 \times T_2)$  vibronic states via anharmonicity.  $A_1$  vibronic states can be differentiated from  $E$  and  $T_2$  based on polarization studies:  $W(A_1)=0$  and  $W(E)=W(T_2)=3/2$ . Such laser polarization effects cannot be found in the presented results. This sug-

gests that either the  $A_1$  vibronic components are very weak or that the Jahn-Teller splitting and coupling in this Rydberg state is very small.

The features observed in the spectrum not assigned to totally symmetric modes above must be due to  $e$ ,  $t_1$ , or  $t_2$  modes. These modes are found in the ground state:<sup>19</sup>  $e$ —427, 912, 1218, 1344, 1460, 2855 cm<sup>-1</sup>;  $t_1$ —309, 886, 1088, 1136, 1328, 1371, 2926 cm<sup>-1</sup>; and  $t_2$ —423, 649, 800, 971, 1109, 1285, 1354, 1439, 2856, 2904, 2932 cm<sup>-1</sup>. Comparison between these frequencies and those observed for the  $T_2$  Rydberg state show little overlap upon which to base assignments. We cannot determine if this is due to Jahn-Teller interactions or simply a substantial ground- to excited-state energy shift.

To summarize these results and analysis for adamantane, the transition observed is  $T_2 \leftarrow A_1 [(\sigma 3s) \leftarrow (\sigma)^2]$ , only three vibronic features in the spectrum can be assigned to totally symmetric vibrations, and vibronically induced  $e$ ,  $t_1$ , and  $t_2$  modes must account for the major non- $0^0$  intensity in this transition. A one-to-one correspondence between the latter excited-state vibrations and the known ground-state modes is not obvious. Polarization ratio studies suggest that the Jahn-Teller effect is small for this excited state: the rigid adamantane cage structure may be responsible for the reduction in vibronic coupling strength in this molecule.

#### IV. CONCLUSIONS

Mass-resolved excitation (2+1) spectra are presented and discussed for cyclohexane ( $H_{12}/D_{12}$ ), bicyclooctane, and adamantane cooled in a supersonic expansion. Cooling techniques have allowed the assigned features for these molecules to be revised. The experimental symmetry assignments for the  $(\sigma 3s) \leftarrow (\sigma)^2$  Rydberg transitions are consistent with predictions of theoretical calculations. With the help of isotopic (H/D) substitution and circular/linear polarization effects, vibronic features are assigned to totally symmetric and vibronically induced modes. The observed two-photon allowed transition for cyclohexane is assigned to  $E_g \leftarrow A_{1g}$  symmetry. Extensive Jahn-Teller coupling must be invoked to interpret the spectrum. The spectrum for adamantane ( $T_2 \leftarrow A_1$ ) is similar in appearance to that of cyclohexane but evidences a much reduced, if present at all, Jahn-Teller coupling. Polarization studies suggest that  $A_1$  vibronic components do not contribute to the observed intensity. The vibronic features in this transition arise through  $e$ ,  $t_1$ , and  $t_2$  mode vibronic coupling. Three totally symmetric modes can

be assigned for the excited state. Bicyclo[2.2.2]octane has two possible electronic transition assignments for the observed allowed two-photon transition. These possibilities are  $A'_1$ ,  $E'' \leftarrow A'_1$ ; they are predicted to be accidentally degenerate. For either Rydberg electronic state symmetry assignment the observed progression forming mode is assumed to be an  $a''_1$  mode whose ground-state energy is 65 cm<sup>-1</sup>. The absence of any obvious Jahn-Teller activity for this system may favor the  $A'_1 \leftarrow A'_1$  assignment with the  $a''_1$  mode at ~30 cm<sup>-1</sup> and the progression in even overtones ( $n=0, 2, 4, 6, 8$ ). The fact that cyclohexane shows a large Jahn-Teller vibronic coupling and adamantane does not is consistent with the rigidity of the two molecules.

#### ACKNOWLEDGMENT

This effort is supported by the U.S. Army Research Office.

- <sup>1</sup>M. B. Robin, *Higher Excited States of Polyatomic Molecules* (Academic, New York, 1977), Vol. 1.
- <sup>2</sup>(a) J. W. Raymonda and W. T. Simpson, *J. Chem. Phys.* **47**, 430 (1967);  
(b) B. A. Lombos, P. Sauvageau, and C. Sandorfy, *J. Mol. Spectrosc.* **24**, 253 (1967); (c) J. W. Caldwell and M. S. Gordon, *Chem. Phys. Lett.* **59**, 403 (1978).
- <sup>3</sup>H. Basch, M. B. Robin, N. A. Kuebler, C. Babor, and D. W. Turner, *J. Chem. Phys.* **51**, 52 (1969).
- <sup>4</sup>J. W. Raymonda, *J. Chem. Phys.* **56**, 3912 (1972).
- <sup>5</sup>B. A. Heath, N. A. Kuebler, and M. B. Robin, *J. Chem. Phys.* **70**, 3362 (1979).
- <sup>6</sup>G. A. Olah and D. R. Squire, *Chemistry of Energetic Materials* (Academic, New York, 1991).
- <sup>7</sup>(a) S. H. Lie, Y. Fujimura, H. J. Neusser, and E. W. Schlag, *Multiphoton Spectroscopy of Molecules* (Academic, New York, 1984); (b) E. R. Bernstein, K. Law, and M. Schauer, *J. Chem. Phys.* **80**, 207 (1984).
- <sup>8</sup>E. B. Wilson, Jr., J. C. Decius, and P. C. Cross, *Molecular Vibrations* (Dover, New York, 1955).
- <sup>9</sup>G. Herzberg, *Electronic Spectra and Electronic Structure of Polyatomic Molecules* (Van Nostrand Reinhold, New York, 1966).
- <sup>10</sup>(a) M. W. McClain and R. A. Harris, *Excited States*, edited by E. C. Lim (Academic, New York, 1977), Vol. 3; (b) M. A. C. Nascimento, *Chem. Phys.* **77**, 51 (1983).
- <sup>11</sup>R. D. Levine and S. G. Lias, *Ionization Potential and Appearance Potential Measurements* (National Bureau of Standards, Washington, D.C., 1971–1981).
- <sup>12</sup>J. MacMurtry, *Organic Chemistry* (Brooks-Cole, City, 1988).
- <sup>13</sup>M. Dupuis and M. Marquez, HONDO 8.4 (IBM, Kingston, NY, 1992).
- <sup>14</sup>K. B. Wiberg and A. Shrake, *Spectrochim. Acta Part A* **29**, 583 (1973).
- <sup>15</sup>J. J. P. Steward, MOPAC, A General Molecular Orbital Package, 6th ed. (U.S. Air Force Academy, 1989).
- <sup>16</sup>J. M. Lehr and G. Wipff, *Theor. Chim. Acta* **33**, 43 (1974).
- <sup>17</sup>P. Bruesch, *Spectrochim. Acta* **22**, 867 (1966).
- <sup>18</sup>W. Schmidt, *Tetrahedron* **29**, 2129 (1973).
- <sup>19</sup>R. T. Bailey, *Spectrochim. Acta Part A* **27**, 1447 (1971).